JOURNAL OF SOLID STATE CHEMISTRY 74, 60–66 (1988)

The Structural and Magnetic Properties of $SrMnO_3$: A Reinvestigation

P. D. BATTLE, T. C. GIBB,* AND C. W. JONES

Department of Inorganic and Structural Chemistry,
The University of Leeds, Leeds LS2 9JT, England

Received September 2, 1987; in revised form November 16, 1987

Neutron diffraction and Mössbauer spectroscopy have revealed that the phase 4H-$SrMnO_3$ is paramagnetic at 290 K, contrary to earlier reports. Mössbauer spectroscopy on ^{57}Fe-doped samples has revealed antiferromagnetic ordering with $T_N = 278 \pm 5$ K. The susceptibility maximum at ~350 K is thought to represent only short-range coupling between Mn^{4+} ions in the Mn_2O_9 pairs of face-sharing octahedra in the structure. © 1988 Academic Press, Inc.

Introduction

There have been many studies of the structural and electronic properties of those mixed metal oxides which are structurally similar to the mineral perovskite, $CaTiO_3$. The interest has often centered on the occurrence of ferromagnetism or antiferromagnetism at relatively high temperatures, the ability of the structure to stabilize cations in unusually high oxidation states, and the ability of the anion sublattice to accommodate a high concentration of vacant sites. Recent studies have begun to explore the consequences of incorporating two different transition metals in a perovskite, for example, $BaFe_{1-x}Mn_xO_{3-\delta}$ (*1*). The crystal structure of all perovskites ABO_3 consists of essentially close-packed layers of stoichiometry AO_3 with the transition metal (B) ions occupying octahedral holes between the layers. The cation A is usually an alkaline earth or lanthanide. Successive AO_3 sheets can be stacked in either *hcp* or *ccp* arrangements, and several mixed stacking sequences are possible (*2*). The consequence of this for the B-site cations is that their coordination octahedra can be linked by either corner sharing or face sharing. Only the former is present in $CaTiO_3$, and only the latter in $BaMnO_3$. In other compounds, for example, 6H-$BaTiO_3$, both face- and corner-sharing octahedra occur in a periodic manner. The occurrence of both arrangements makes the prediction of magnetic properties more difficult, and if two transition metals are present, as in $BaFe_{1-x}Mn_xO_{3-\delta}$, then there is the additional complication that the two different elements might be ordered or disordered over the two types of site.

Mixed valency, caused by an oxide sublattice that is only partially occupied ($\delta > 0$) extends the range of possibilities still further. We are currently engaged in a study of the structural and magnetic properties of

---

* To whom correspondence should be addressed.

0022-4596/88 $3.00

the mixed systems $SrMn_{1-x}Fe_xO_{3-\delta}$ and $SrMn_{1-x}Co_xO_{3-\delta}$, and as part of our work we prepared a sample of the end-member $SrMnO_3$. It has been established (*3*) that $SrMnO_3$ has a hexagonal unit cell, the dimensions of which (a_0 = 5.449 Å, c_0 = 9.078 Å) indicate a mixed hexagonal/cubic close-packing of the AO_3 layers such that the structure consists of pairs of face-sharing octahedra, these Mn_2O_9 units being linked by corner sharing. An X-ray diffraction study has been carried out (*4*) on a single crystal of nominal stoichiometry $SrMnO_3$, although no chemical analysis was reported, and the structure of the related compound $Sr_{0.9}Ba_{0.1}MnO_{2.96}$ has been refined using neutron diffraction data collected at 4.2 K (*5*). In this paper we use room temperature neutron diffraction and Mössbauer data to identify a misinterpretation of the magnetic susceptibility data collected previously (*6*). Those data, having a maximum value at ~350 K, led Chamberland *et al.* (*6*) to propose that $SrMnO_3$ orders antiferromagnetically with T_N = 350 K. Our own data indicate that this is incorrect, and we offer an alternative explanation for the observed temperature dependence of the magnetic susceptibility.

Experimental

A polycrystalline sample of $SrMnO_3$ was prepared by firing stoichiometric quantities of spectroscopic-grade $SrCO_3$ and MnO_2 in pellet form at 1250°C for a total of 7 days and then at 1350°C for a total of 13 days with several intermediate grindings. The sample was finally cooled to 500°C at a rate of only 50°/hr to maximize the oxygen content before quenching to room temperature. The composition of the reagent MnO_2 was verified both gravimetrically and by iodometric titration. The latter method established the stoichiometry of the final product as $SrMnO_{2.993}$ and X-ray powder diffraction suggested that it was isostructural with the 4H-$SrMnO_3$ described by Negas and Roth (*3*), as would be expected in view of the conditions of synthesis employed. A second sample was prepared in a similar manner, except that $^{57}Fe_2O_3$ was used to substitute ^{57}Fe for ~1.3% of the Mn cations.

The magnetic susceptibility of the original sample was measured as a function of temperature for $80 < T < 300$ K, the widest range available, using a Newport Instruments Gouy balance. Neutron diffraction data were collected at room temperature using the powder diffractometer D1a at ILL Grenoble, operating at a wavelength of 1.956 Å. The bank of 10 counters was moved in steps of 0.05° in order to scan the range $6 < 2\theta < 150°$ over a period of 12 hr. The sample was contained in a vanadium can. Mössbauer data were collected in the temperature range $4.2 < T < 290$ K using a ^{57}Co/Rh source matrix held at room temperature; isomer shifts were determined relative to the spectrum of metallic iron.

Results and Discussion

The results of our magnetic susceptibility measurements are shown in Fig. 1. They are very similar, in both magnitude and temperature dependence, to those reported previously by Chamberland *et al.* (*6*) and they are consistent with $SrMnO_3$ having a Néel temperature above 300 K. However, this is not a unique interpretation of the results and we shall show below that it is in fact incorrect.

The Mössbauer spectrum of ^{57}Fe/$SrMnO_3$ recorded at 290 K is shown in Fig. 2. The absorption is asymmetric, suggesting the presence of both Fe^{4+} and Fe^{3+} in the sample, but there is no magnetic hyperfine splitting, thus demonstrating that there is no long-range magnetic ordering in $SrMnO_3$ at this temperature. The very low concentration of ^{57}Fe in the sample means that the Néel temperature will not be significantly different to that of undoped

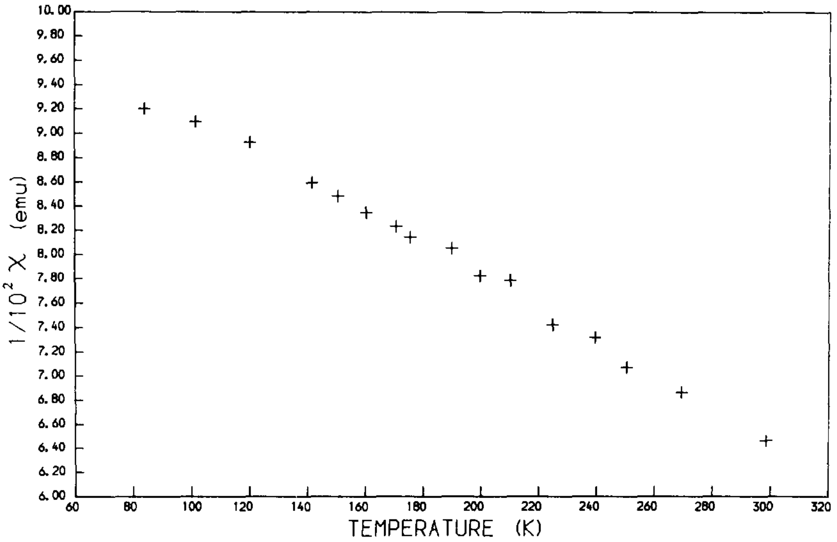

FIG. 1. Temperature dependence of the inverse molar susceptibility of $SrMnO_3$.

$SrMnO_3$. The spectrum has strong similarities to that for the mixed-valence perovskite $SrFeO_{2.844}$ which has been described elsewhere (7), the main difference being that the Fe^{3+} component does not show such a significant quadrupole splitting. The observed spectrum was analyzed in terms of a quadrupole-split doublet from Fe^{4+}, the two components being constrained to have equal linewidths and intensities, and a singlet from Fe^{3+}. Alternative analyses produced no positive evidence for a significant quadrupole splitting of the Fe^{3+} component. The resulting parameters are presented in Table I. The presence of an absorption due to Fe^{3+} indicates that the ^{57}Fe-doped sample deviates from the ideal stoichiometry, as did the undoped sample.

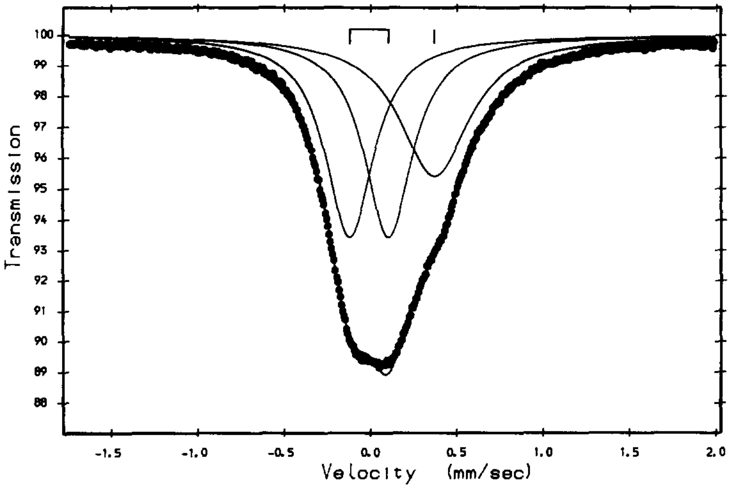

FIG. 2. Observed (...) and calculated (—) ^{57}Fe Mössbauer spectrum of $^{57}Fe/SrMnO_3$ at 290 K.

TABLE I

MÖSSBAUER PARAMETERS FOR ^{57}Fe/SrMnO$_3$ AT 290 K

Cation	δ (mm sec^{-1})	Δ (mm sec^{-1})	Γ (mm sec^{-1})	% Area
Fe^{3+}	0.37	0	0.49	34
Fe^{4+}	−0.01	0.22	0.34	66

TABLE II

MÖSSBAUER PARAMETERS FOR ^{57}Fe/SrMnO$_3$ AT 4.2 K

Cation	δ (mm sec^{-1})	B (T)	Γ_0 (mm sec^{-1})	Γ_{eff} (mm sec^{-1})	% Area
Fe^{3+}	0.22	44.1	0.40	2.59	48
Fe^{4+}	−0.07	30.5	0.40	1.90	52

Variable temperature Mössbauer spectroscopy allowed us to observe the appearance of two overlapping six-line spectra somewhat below room temperature and thus to estimate the Néel temperature for long-range antiferromagnetic ordering in SrMnO$_3$ as 278 ± 5 K. The magnetically saturated six-line spectrum observed at 4.2 K is shown in Fig. 3, and the computer-fitted spectral parameters are presented in Table II. They represent a model in which two overlapping magnetic hyperfine sextets were used to fit the data, each being defined by an independent isomer shift and hyperfine field. The quadrupole splittings are too small to significantly effect these magnetic hyperfine splittings and were assumed to be zero, and the intensities of the six lines were constrained to be in the ideal ratios 3 : 2 : 1 : 1 : 2 : 3 expected for a randomly orientated powdered sample. It became clear during data analysis that the outer lines in the spectrum are exceptionally broad. It is necessary to assume that a range of hyperfine fields is present at both the ^{57}Fe sites in the structure. This was accommodated in a simplified model as follows. The linewidth of line n, Γ_n, was defined to be $\Gamma_n = \Gamma_0(1 + p_n\Gamma_{eff})$ where p_n is the fractional displacement of the nth line along the baseline from the centroid of the sextet (thus $p_n = 0.1578$ for $n = 3$ or 4, $= 0.5789$ for $n = 2$ or 5, $= 1$ for $n = 1$ or 6). The value of Γ_0 was constrained to be the same for both sextets but Γ_{eff} was varied independently for each pattern. The sextet due to Fe^{3+} ($\delta = 0.217$ mm sec^{-1}) and that due to Fe^{4+} ($\delta = -0.066$ mm sec^{-1}) are both significantly broadened, and

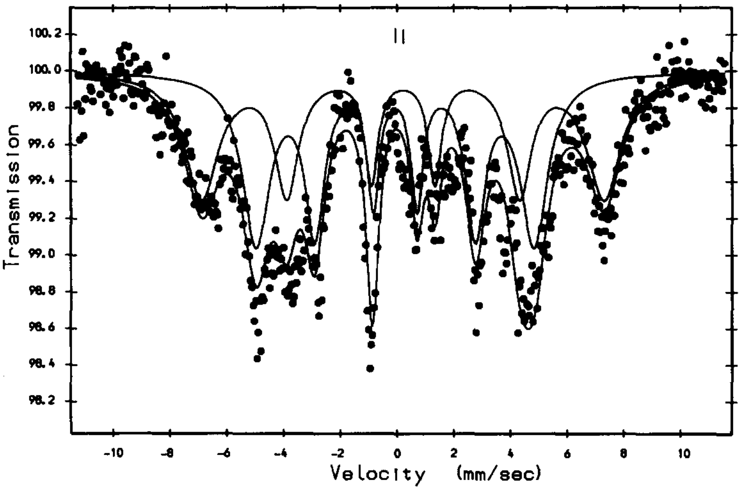

FIG. 3. Observed (...) and calculated (—) ^{57}Fe Mössbauer spectrum of ^{57}Fe/SrMnO$_3$ at 4.2 K.

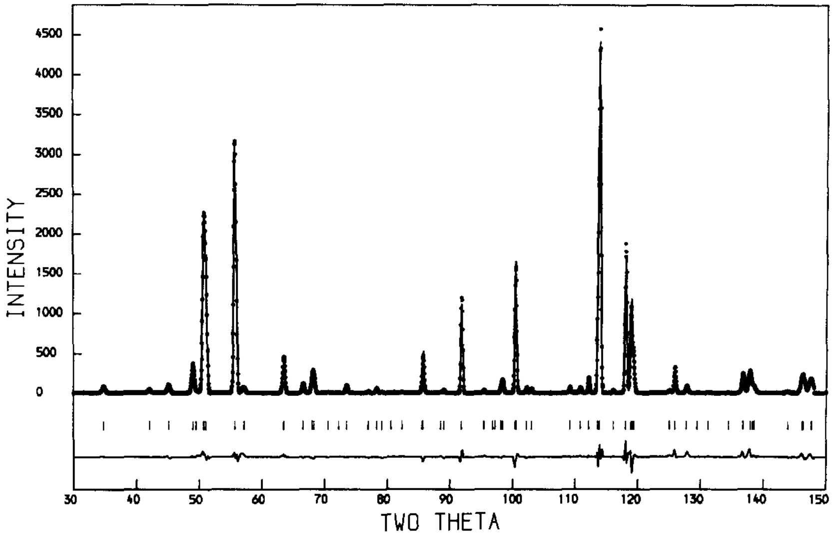

FIG. 4. Observed (...), calculated (—), and difference neutron diffraction profiles for $SrMnO_3$ at 290 K. Reflection positions are marked.

this may be due to the location of anion vacancies in the immediate vicinity of the dopant. The comparatively high proportion of Fe^{3+} observed is also suggestive of extensive defect association. The flux densities of the hyperfine fields of 44.1 and 30.5 T for Fe^{3+} and Fe^{4+}, respectively, are comparable with the values of 45.6, 44.1, and 29.3 T for the same oxidation states in $SrFeO_{2.844}$ (*7*) and lend confidence to the assignment. Because of unknown variations in the recoilless fractions, and the undoubted limitations of the two simple models we have applied to two complex absorption patterns, the apparent change in the relative areas of the two patterns between room temperature and 4.2 K is probably not significant.

Our neutron diffraction results confirm that $SrMnO_3$ is paramagnetic at room temperature. All the observed diffraction peaks could be indexed in space group $P6_3/mmc$ with unit cell parameters a_0 = 5.4434(2), c_0 = 9.0704(1) Å. The crystal structure was refined using the Rietveld profile analysis method (*8*) taking the structure of $Sr_{0.9}Ba_{0.1}MnO_{2.96}$ as a starting model (*5*). Data with $2\theta < 30°$ were excluded from the final refinement because of asymmetric peak shapes, and 59 Bragg reflections were then used to refine two positional parameters, five isotropic temperature factors, and seven profile parameters. No additional scattering that could be magnetic in origin was observed and the refinements converged to give an agreement factor R_{wpr} = 10.3%. The observed, calculated, and difference profiles are plotted in Fig. 4 and the refined structural parameters are listed in Table III. Bond distances and bond angles are given in Table IV, and a fragment of the structure is drawn in Fig. 5. The tabulated

TABLE III

ATOMIC COORDINATES AND TEMPERATURE FACTORS FOR $SrMnO_3$ AT 290 K (SPACE GROUP $P6_3/mmc$)

Atom	Site	x	y	z	B (Å^2)
Sr1	2a	0	0	0	0.31(7)
Sr2	2c	$\frac{1}{3}$	$\frac{2}{3}$	$\frac{1}{4}$	0.49(6)
Mn	4f	$\frac{1}{3}$	$\frac{2}{3}$	0.6122(5)	0.16(5)
O1	6g	$\frac{1}{2}$	0	0	0.95(4)
O2	6h	−0.1807(2)	−0.3614(4)	$\frac{1}{4}$	0.23(4)

TABLE IV

BOND DISTANCES (IN Å) AND BOND ANGLES (IN °) FOR $SrMnO_3$ AT 290 K

Sr(1)–O(1)	2.722
Sr(1)–O(2)	2.836(5)
Sr(2)–O(1)	2.759
Sr(2)–O(2)	2.725(5)
Mn–O(1)	1.872(5)
Mn–O(2)	1.906(7)
Mn–Mn	2.500(6)
O(1)–Mn–O(1)	93.25
O(1)–Mn–O(2)	92.27
O(2)–Mn–O(2)	81.66
Mn–O(2)–Mn	81.95
Mn–O(1)–Mn	180.00

data show no significant differences between the structure of $SrMnO_3$ and that of $Sr_{0.9}Ba_{0.1}MnO_{2.96}$ reported previously by Jacobson and Horrox (*5*) (note that Figs. 3 and 4 are incorrectly labeled in the earlier work). Kuroda *et al.* (*4*) invoked a disordered arrangement of Sr1 about the origin in order to account for their observed X-ray diffraction data; our refinements did not improve significantly when we allowed Sr1 to occupy $(0,0,\pm z)$ positions but we cannot rule out the possibility of a statistical distribution of cations about (0,0,0). The atomic coordinates in Table III are otherwise in good agreement with those of Kuroda *et al.* (*4*) although the temperature factors refined to significantly lower values in the present work.

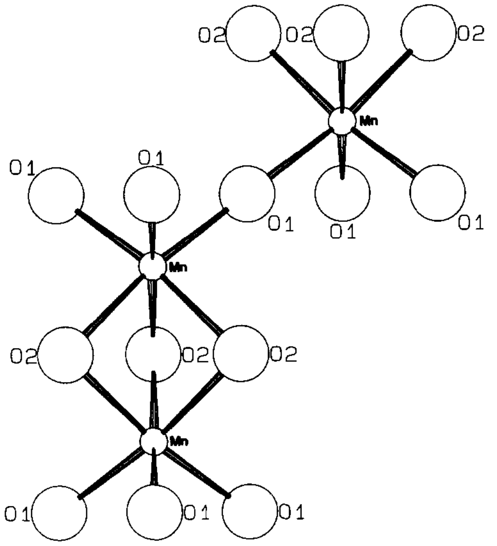

FIG. 5. A structural fragment of $SrMnO_3$ illustrating the two different types of polyhedra linkage.

We must reconcile the susceptibility data of Fig. 1 with the Mössbauer spectrum of Fig. 2 and the neutron diffraction pattern of Fig. 4. The latter two results prove that there is no long-range magnetic ordering at 290 K in $SrMnO_3$, yet the former show a maximum at ~350 K. We believe that short-range antiferromagnetic coupling is taking place between the two Mn^{4+} ions in the Mn_2O_9 clusters below ~350 K, but that the intercluster superexchange is not strong enough to establish long-range antiferromagnetism until ~278 K. It is entirely reasonable that the interaction between two d^3 cations in face-sharing octahedra should be stronger than between the same cations in corner-sharing octahedra, and our results illustrate the pitfalls that can occur when susceptibility data alone are used in the magnetic characterization of materials which contain both types of polyhedra linkage.

Acknowledgments

We thank the SERC for financial support, including a postgraduate studentship for C.W.J., and Dr. A. W. Hewat for assistance at ILL Grenoble.

References

1. V. CAIGNAERT, M. HERVIEU, B. DOMENGES, N. NGUYEN, J. PANNETIER, AND B. RAVEAU, "Abstracts of the Third European Conference on Solid State Chemistry," Vol. III, Regensburg (1986).

2. A. L. Patterson and J. S. Kasper, *in* "International Tables for X-ray Crystallography," Vol. II, Kynoch Press, Birmingham (1959).
3. T. Negas and R. S. Roth, *J. Solid State Chem.* **1,** 409 (1970).
4. K. Kuroda, N. Ishizawa, N. Mizutani, and M. Kato, *J. Solid State Chem.* **38,** 297 (1981).
5. A. J. Jacobson and A. J. W. Horrox, *Acta Crystallogr. Sect. B* **32,** 1003 (1976).
6. B. L. Chamberland, A. W. Sleight, and J. F. Weiher, *J. Solid State Chem.* **1,** 506 (1970).
7. T. C. Gibb, *J. Chem. Soc. Dalton Trans.,* 1455 (1985).
8. H. M. Rietveld, *J. Appl. Crystallogr.* **2,** 65 (1969).